Acid property of MFI-type zeolites probed by trimethylphosphine oxide studied by solid-state NMR

Shigenobu Hayashi *, Keiko Jimura, Natsuko Kojima

Research Institute of Instrumentation Frontier, National Institute of Advanced Industrial Science and Technology (AIST), Tsukuba Central 5, 1-1-1 Higashi, Tsukuba, Ibaraki 305-8565, Japan

ABSTRACT

Acid properties of ZSM-5 type zeolite are studied by solid-state NMR using trimethylphosphine oxide (TMPO) as a probe molecule. TMPO is introduced from the gas phase at 373 K. The amounts of the loaded TMPO are quantified by the signal intensities of ^{1}H MAS NMR spectra, which are compared with the numbers of Brønsted acid sites estimated by the Si/A ratio of the framework derived from ^{29}Si MAS NMR spectra and the content of fourfold-coordinated Al from ^{27}Al MAS NMR spectra. The use of 373 K for loading the probe molecules increases the loading level of TMPO, and thus almost all the acid sites are probed. The ^{31}P chemical shifts in the range between 90 and 60 ppm are attributed to TMPO adsorbed on Brønsted acid sites, whereas the signals between 60 and 40 ppm are ascribed to TMPO adsorbed on other sites than Brønsted acid sites. The ^{13}C chemical shift of methyl groups in the adsorbed TMPO depends mainly on the confined space as well as on the acid strength.

© 2013 Elsevier Inc. All rights reserved.

1. Introduction

Trimethylphosphine oxide (TMPO) is frequently used to probe surface acidity in the field of solid-state NMR [1–14], because ^{31}P has high sensitivity and the ^{31}P chemical shift of TMPO is sensitive to the acid strength. TMPO is a solid substance at room temperature, whose melting point is about 413 K. Anhydrous tetrahydrofuran and dichloromethane have been used as a solvent when TMPO is adsorbed. After introduction of the TMPO solution, the solvent was removed by evacuation. However, we found that some samples adsorb the solvent molecules as strongly as TMPO [15,16]. For those samples, the solvent molecules cannot be removed without desorption of a part of TMPO.

In the previous works, we proposed a method to introduce TMPO from the gas phase in order to avoid the effect of the solvents, and then applied the vapor method to H-type mordenite [15,17]. TMPO was introduced from the gas phase at room temperature, and ^{31}P NMR spectra of adsorbed TMPO were successfully traced. However, the concentration of the adsorbed TMPO was too small to probe all acid sites. Furthermore, a dominant fraction of the adsorbed TMPO was physisorbed.

In the present work, the vapor method has been improved by raising the sample temperature. The samples studied were H-type ZSM-5 zeolite, which has an MFI-type framework with the channel sizes of 0.55×0.51 nm^2 and 0.56×0.53 nm^2 [18]. H-type ZSM-5

adsorbs dichloromethane as strongly as TMPO, and thus the solvent method is not adequate [16]. ^{31}P NMR spectra of the adsorbed TMPO were measured for the samples prepared by the improved vapor method. ^{1}H and ^{13}C NMR spectra were also measured to obtain information on the adsorbed probe molecules. We discuss dependences of the state of TMPO on the concentration of the adsorbed TMPO and the Si/Al ratio of the framework.

2. Experimental

2.1. Materials

TMPO was obtained from Alfa Aesar (USA). ZSM-5 zeolite samples were supplied by The Catalysis Society of Japan. They were coded as JRC-Z5-25H, JRC-Z5-70H and JRC-Z5-70Na. JRC means Japan Reference Catalyst and Z5 is ZSM-5. The number is a nominal SiO$_2$/Al$_2$O$_3$ molar ratio. H and Na attached to the number mean H$^+$ and Na$^+$ forms, respectively. The as-supplied JRC-Z5-25H sample contained NH$_4^+$ ions and, therefore, the sample was calcined at 808 K under an air atmosphere to convert to H$^+$ form. JRC will be removed in the following description.

2.2. Adsorption of TMPO

TMPO was adsorbed from the gas phase. The vapor method previously used [15,17] was improved for the purposes of avoiding the contact with atmospheric moisture and accelerating the diffusion

---

* Corresponding author. Tel./fax: +81 29 861 9333.
  E-mail address: hayashi.s@aist.go.jp (S. Hayashi).

of the probe molecules into the micopores. The procedures were as follows. The host sample was put in a glass tube with a stopcock and evacuated. Under dynamic vacuum conditions the sample temperature was raised gradually and then kept at 473 K for 3 h to remove adsorbed water. After cooling to room temperature, a known amount of solid TMPO was added to the host sample under an N_2 atmosphere. The glass tube containing the host and TMPO was evacuated with an oil rotary vacuum pump at room temperature. The glass tube was isolated from the vacuum line by a stopcock, and then heated at 373 K for 3 h. The TMPO-loaded sample was gradually cooled to room temperature.

The prepared samples were carefully handled without exposure to an air atmosphere. All the samples were packed into a magic-angle-spinning (MAS) rotor under an N_2 atmosphere using a glovebag. After packing into the rotor, the sealing of the 4-mm MAS rotor was rather good [19].

2.3. NMR measurements

MAS NMR spectra of ^{29}Si, ^{27}Al, ^{1}H, ^{31}P and ^{13}C were measured at room temperature with a Bruker ASX400 spectrometer at Larmor frequencies of 79.49, 104.26, 400.13, 161.98 and 100.61 MHz, respectively. A Bruker MAS probehead was used with a zirconia rotor of a 4.0-mm outer diameter, except for the ^{29}Si measurements where the outer diameter of the rotor was 7.0 mm. The pulse sequence was a single-pulse sequence with ^{1}H high-power decoupling during signal acquisition (HD) for ^{29}Si, ^{27}Al, ^{31}P and ^{13}C. The parameters used were a $\pi/4$ pulse and a repetition time of 10 s for ^{29}Si, a $\pi/14$ pulse and a repetition time of 1 s for ^{27}Al, a $\pi/4$ pulse and a repetition time of 7 s for ^{31}P, a $\pi/2$ pulse and a repetition time of 3 s for ^{13}C. The small flip angle of the ^{27}Al pulse was used to ensure the quantitative nature of the signal intensity of the quadrupole nucleus [20]. The ordinary single-pulse sequence (SP) was used for ^{1}H, where the parameters were a $\pi/2$ pulse and a repetition time of 6 s. In the case of ^{29}Si, the cross polarization (CP) pulse sequence was also used in addition to ^{1}H high-power decoupling during signal acquisition. The flip angle of the initial ^{1}H pulse was $\pi/2$, the contact time was 5 ms, and the repetition time was 1 s. The frequency scales of the ^{29}Si, ^{27}Al, ^{1}H, ^{31}P and ^{13}C spectra were expressed with respect to neat tetramethylsilane by adjusting the strongest signal of sodium 3-(trimethylsilyl)propionate to 1.459 ppm [21], 1.0 M Al(NO$_3$)$_3$ aqueous solution by adjusting the signal of AlNH$_4$(SO$_4$)$_2$·12H$_2$O to −0.54 ppm [22], neat tetramethylsilane (TMS) by adjusting the signal of adamantane spinning at 8.0 kHz to 1.87 ppm [23], 85% H$_3$PO$_4$ aqueous solution by adjusting the signal of (NH$_4$)$_2$HPO$_4$ to 1.33 ppm [22] and neat tetramethylsilane by adjusting the lower-frequency signal of adamantane to 29.472 ppm [21], respectively.

The signal intensities of the ^{27}Al and ^{1}H NMR spectra were analyzed quantitatively by using external reference materials, AlNH$_4$(SO$_4$)$_2$·12H$_2$O and adamantine for ^{27}Al and ^{1}H, respectively.

3. Results and discussion

3.1. ^{29}Si and ^{27}Al MAS NMR spectra of host samples

Fig. 1 shows ^{29}Si MAS NMR spectra of Z5-25H and Z5-70H. The samples were equilibrated with water by keeping them in a space with 100% humidity at room temperature. The HD/MAS NMR spectra consist of several Si(nAl) components, where Si(nAl) means an Si atom connected with nAl atoms via an O atom. On the other hand, the signal intensities of the CP/MAS NMR spectra are much smaller than the corresponding HD/MAS NMR spectra. The CP technique enhances the signal intensity of ^{29}Si near ^{1}H such as Si–OH. The signal intensities of the CP/MAS spectra are normalized
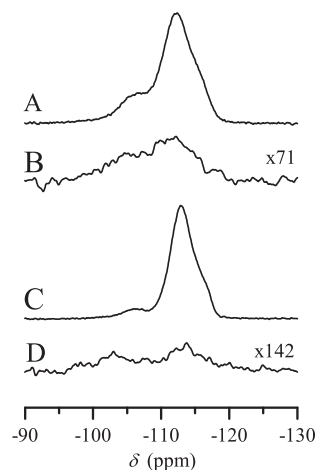

Fig. 1. ^{29}Si MAS NMR spectra of hydrated samples of (A,B) Z5-25H and (C, D) Z5-70H. The pulse sequences were (A, C) HD and (B, D) CP. The signal intensities for the same samples are normalized, and the CP spectra are enlarged by the numbers in the figure. The spinning rate of the sample was 4 kHz.

by taking into account the excitation pulse length and assuming an ideal CP efficiency. The remarkably low intensity of the CP spectra shown in Fig. 1 demonstrates that the concentration of Si–OH can be neglected in the estimation of the framework Si/Al ratio. The HD/MAS spectra are deconvoluted into several components, assuming Gaussian line shapes. Table 1 summarizes the deconvolued results. The Si/Al atomic ratios of the framework are estimated from the results in Table 1, assuming Loewensten's rule. The framework Al contents are estimated from the Si/Al ratio, which are equal to the contents of Brønsted acid sites. Table 1 also lists the Si/Al ratio and the framework Al contents.

Fig. 2 shows ^{27}Al MAS NMR spectra of the hydrated samples of Z5-25H and Z5-70H. Two signals are observed at about 54 and −2 ppm, which are ascribed to fourfold-coordinated Al (AlO$_4$) and sixfold-coordinated Al (AlO$_6$), respectively. The former is framework Al, while the latter is non-framework Al. Those signals have a tail at the lower frequency side. The Al contents are evaluated from the signal intensity of the ^{27}Al MAS NMR spectra. Table 2 summarizes the results. The framework Al contents evaluated from the ^{27}Al results agree fairly well with those from the ^{29}Si results.
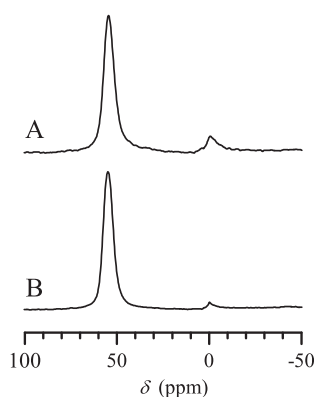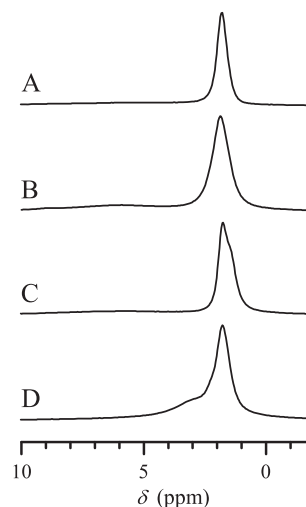
3.2. ^{1}H MAS NMR spectra of TMPO-adsorbed samples

Fig. 3 shows ^{1}H MAS NMR spectra of TMPO-adsorbed samples. The relatively sharp peak at 1.8 ppm is ascribed to methyl group (CH$_3$) of TMPO. The signal intensities of TMPO are quantitaively analyzed, and the contents of the adsorbed TMPO are evaluated, as shown in Table 3.

The content of TMPO in the sample of Z5-25H (TMPO content of 0.42 mmol/g) is less than the amount of Brønsted acid sites, while that in Z5-25H (1.64 mmol/g) exceeds the number of Brønsted acid sites. The loading amount for Z5-70H is 0.14 mmol/g, which is less than the number of Brønsted acid sites, 0.5 mmol/g. The loading amount for Z5-70Na is 0.23 mmol/g, although the Na-type sample has a negligible amount of Brønsted acid sites.

A TMPO-loaded Z5-25H sample was also prepared by the solvent method for reference. The preparation method is described in Supplementary data. The ^{1}H MAS NMR spectrum consists of two peaks at 5.5 and 2.0 ppm (See Fig S1 in Supplementary data). The former is ascribed to the CH$_2$Cl$_2$ solvent, and the latter is to TMPO. The ^{1}H signal of Brønsted acid sites is spread underneath the above signals without clear peaks. The CH$_2$Cl$_2$ solvent remains undesorbed, as reported previously [16]. Consequently, the vapor method is more adequate than the solvent method for the present system.

Table 1
29Si MAS NMR results of the hydrated host samples.

Sample	29Si chemical shift (ppm) [Fraction (%)]			Si/Al atomic ratio [a]	Al_F [b] (mmol/g)
	Si(2Al)	Si(1Al)	Si(0Al)		
Z5-25H	−99.7 [2.5]	−106.5 [22.0]	−112.2 [60.1]	14.8	1.05
			−115.8 [15.3]		
Z5-70H	−99.5 [0.8]	−106.9 [12.6]	−112.9 [74.2]	28.2	0.57
			−116.3 [12.4]		

[a] The error is ±20%.
[b] Framework Al contents, being estimated from the Si/Al ratio, which are equal to the contents of Brønsted acid sites. The error is ±20%.

Fig. 2. 27Al HD/MAS NMR spectra of hydrated samples of (A) Z5-25H and (B) Z5-70H. The spinning rate was 10 kHz.

3.3. 31P MAS NMR spectra of TMPO-adsorbed samples

Fig. 4 shows 31P MAS NMR spectra of the TMPO-adsorbed Z5-25H samples. At a loading level of 0.42 mmol/g, the signals spread in the range between 90 and 60 ppm. At the high loading level of 1.64 mmol/g, the signals cover the range between 80 and 40 ppm. Fig. 5 shows 31P MAS NMR spectra of the TMPO-adsorbed samples of Z5-70H and Z5-70Na. The signals cover the range between 80 and 35 ppm and between 60 and 40 ppm for Z5-70H and Z5-70Na, respectively.

The spectra are deconvoluted into several components, assuming Gaussian line shapes. The components consisting of the spectra are shown in Figs. 4 and 5 by dotted lines, and Table 3 summarizes the deconvoluted results. The contents of TMPO for each signal are listed also in Table 3, being estimated from the total TMPO contents obtained by the 1H MAS NMR spectra and the fraction of each component obtained by the 31P MAS NMR spectra.

The spin–lattice relaxation times, T_1, of 31P are 6.3 and 1.7 s for crystalline and hydrated TMPO [19]. We used a $\pi/4$ pulse and a repetition time of 7 s for 31P measurements. The signal saturation is considered to be very small, because the adsorbed TMPO is likely to hydrated TMPO from the spinning sideband intensities. Furthermore, the relative intensities of the components are not so affected by the repetition time, because they are only affected by the variation of the T_1 values of each component.

Fig. 3. 1H SP/MAS NMR spectra of TMPO-adsorbed samples. (A) Z5-25H (TMPO loading of 0.42 mmol/g), (B) Z5-25H (1.64 mmol/g), (C) Z5-70H (0.14 mmol/g) and (D) Z5-70Na (0.23 mmol/g). The spinning rates were (A, C) 8 kHz and (B, D) 10 kHz.

Zhao et al. observed seven distinct 31P peaks at 86, 75, 67, 63, 53, 43 and 30 ppm for H-ZSM-5 zeolites [6], as listed in Table 3. The signals at 86, 75, 67, 63 and 53 ppm were ascribed to TMPO adsorbed on Brønsted acid sites [6]. The signal at 43 ppm was assigned to physisorbed TMPO, while that at 30 ppm was to "mobile" TMPO [6]. The present study shows the presence of similar signals except for that at 30 ppm, although the deconvolution process produces excess signals at about 82, 71 and 58 ppm. Among the above signals, the assignment of the 53-ppm signal was somewhat controversial. Baltusis et al. assigned the signal to TMPO associated with Lewis acidity [1], whereas Rakiewicz et al. [2] and Zhao et al. [6] assigned it to TMPO adsorbed on Brønsted acid sites [2]. The latter groups compared TMPO results with trimethylphosphine (TMP) data, and denied the possibility of Lewis acidity.

In the present work, we have attempted to change the loaded amount of TMPO, as shown in Fig. 4 for Z5-25H. With increase in the TMPO concentration, the 31P signal tends to shift towards the lower frequency. This can be interpreted by that TMPO prefers the stronger acid sites. The amount of Brønsted acid sites is about 1.1 mmol/g. The quantitative analysis summarized in Table 1

Table 2
Al contents in the host samples, estimated from 27Al MAS NMR.

| Sample	Hydrated Total Al (mmol/g)[a]	H2O content [b] (mass%)	Dehydrated (mmol/g)		
			TotalAl [c]	AlO_4 [c]	AlO_6 [c]
Z5-25H	1.22	10.3	1.36	1.20	0.16
Z5-70H	0.48	11.9	0.54	0.52	0.02

[a] The error is ±20%.
[b] The mass loss due to H2O desorption measured by thermogravimetric (TG) analysis.
[c] Dried-host basis. The error is ±20%.

Table 3
The ^{31}P chemical shift and the content of adsorbed TMPO.

Host	Z5-25H	Z5-25H	Z5-70H	Ref. [6]	Z5-70Na
TMPO content[a] (mmol/g)	0.42	1.64	0.14		0.23
^{31}P chemical shift (ppm) [content (mmol/g)]	86.4 [0.015]			86	
	82.4 [0.043][b]	81.3 [0.093][b]			
	77.1 [0.16]	76.0 [0.46]	75.9 [0.062]	75	
	72.1 [0.071][b]	70.5 [0.17][b]	69.9 [0.009][b]		
	68.2 [0.070]	65.0 [0.55]	65.1 [0.017]	67	
	65.9 [0.016]				
	63.9 [0.049]		61.9 [0.002]	63	
			57.6 [0.015][b]		56.7 [0.11]
		52.4 [0.36]	51.6 [0.004]	53	
			47.3 [0.017]		48.3 [0.076]
					43.8 [0.009]
					43.6 [0.032][b]
			40.7 [0.011]	43	
			37.1 [0.004]		
				30	

[a] Estimated from the ^{1}H NMR signal intensity. The error is ±20%.
[b] No clear peaks in the observed spectra.
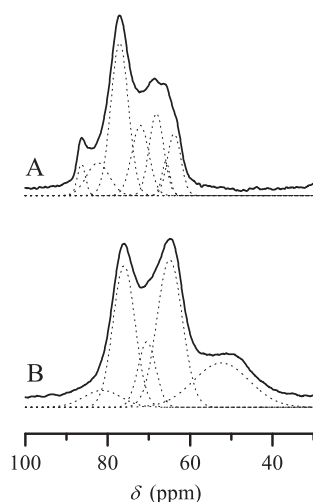
Fig. 4. ^{31}P HD/MAS NMR spectra of TMPO-adsorbed Z5-25H samples. The amounts of the loaded TMPO were (A) 0.42 and (B) 1.64 mmol/g. The spinning rates were (A) 8 kHz and (B) 10 kHz. The dotted lines are the deconvoluted components.
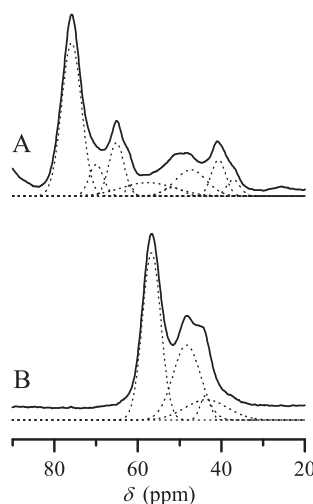
Fig. 5. ^{31}P HD/MAS NMR spectra of TMPO-adsorbed samples. (A) Z5-70H (TMPO loading of 0.14 mmol/g) and (B) Z5-70Na (0.23 mmol/g). The spinning rates were (A) 8 kHz and (B) 10 kHz. The dotted lines are the deconvoluted components.

suggests that TMPO adsorbed on Brønsted acid sites has ^{31}P signals in the range between 90 and 60 ppm and that the signals between 60 and 40 ppm are ascribed to TMPO adsorbed on other sites than Brønsted acid sites. The assignment of the 53-ppm signal to Brønsted acid sites in previous works is not supported by the quantitative analysis of the present work. Almost all Brønsted acid sites are probed by TMPO in the present loading conditions. The previous work did not try to change the TMPO content, and only 54–70% of the total Brønsted acid sites were detected [6]. The solvent method was used in the previous work.

Zhao et al. reported that the relative intensity of the higher-frequency signal increased upon increasing the Si/Al ratio [6]. The same trend is also observed in the present work. This means that the average acid strength increases with the Si/Al ratio. On the other hand, the absolute total concentration of the acid site decreases with increase in the Si/Al ratio. Thus, the absolute concentration of the stronger acid sits does not increase with increase in the Si/Al ratio, as listed in Table 1.

The Na-type sample Z5-70Na does not have signals in the range higher than 60 ppm. Those signals ranging from 60 to 40 ppm are not ascribed to TMPO adsorbed on Brønsted acid sites. They are interacting with Na$^+$ ions and/or the framework. Water molecules might also interact with TMPO, because a ^{1}H signal is observed at 3.1 ppm. This signal position of 3.1 ppm suggests that the water molecules are partially isolated. Bulk water with hydrogen bond networks has a ^{1}H chemical shift of 4.877 ppm [21].

In the previous work, TMPO was introduced from the gas phase at room temperature on H-type mordenite [17]. The concentration of the adsorbed TMPO was too small, and physisorbed TMPO was dominant, which had a ^{31}P chemical shift of 46 ppm [17]. The channel size of ZSM-5 is smaller than that of mordenite. Despite the smaller channel size, TMPO can successfully probe the acid sites in the channels of ZSM-5 in the present work. The loading temperature used in the present work (373 K) accelerates the diffusion of the probe molecules in the channels.

The ^{31}P MAS NMR spectra of the TMPO-loaded Z5-25H sample prepared by the solvent method were measured for comparison (See Fig S2 in Supplementary data). The deconvoluted result is summarized in Table S1 in Supplementary data. The spectrum is similar to that of Z5-25H (0.42 mmol/g) prepared by the vapor method, although crystalline TMPO coexists. The loading temperatures in the solvent method and the vapor method are room temperature and 373 K, respectively. The difference in the loading temperature affects the distribution of the probe molecules in the micropores.
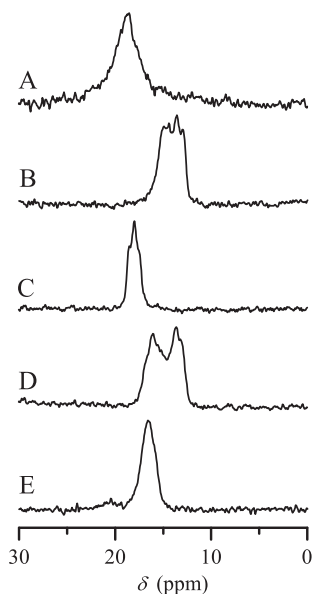
Fig. 6. ^{13}C HD/MAS NMR spectra of (A) Crystalline TMPO and TMPO-adsorbed samples; (B) Z5-25H (0.42 mmol/g), (C) Z5-25H (1.64 mmol/g), (D) Z5-70H (0.14 mmol/g) and (E) Z5-70Na (0.23 mmol/g). The spinning rates were 4 kHz.

3.4. ^{13}C MAS NMR spectra of TMPO-adsorbed samples

Fig. 6 shows ^{13}C HD/MAS NMR spectra of crystalline TMPO and the TMPO-adsorbed samples. The signal position of methyl groups depends on the sample. Crystalline TMPO has a signal at 18.8 ppm, which is the highest frequency among the samples. The Z5-25H sample with TMPO loading of 0.42 mmol/g shows signals at 14.9, 14.4, 13.6 and 13.0 ppm, while Z5-25H (1.64 mmol/g) has signals around 18.0 ppm. The Z5-70H sample (0.14 mmol/g) shows signals around 16.1 and 13.6 ppm. Z5-70Na (0.23 mmol/g) has signals around 16.6 ppm. Some spectra have fine structures, which are caused by indirect spin–spin coupling between ^{13}C and ^{31}P.

Taking into consideration the ^{31}P NMR results, the ^{13}C signals are assigned as follows: The signals at 15–13 ppm are ascribed to TMPO adsorbed on Brønsted acid sites, being supported by the ^{31}P NMR spectra. Combining the results of ^{13}C NMR (Figs. 6B and 6D) and ^{31}P NMR (Figs. 4A and 5A) of Z5-25H (0.42 mmol/g) and Z5-70H (0.14 mmol/g) indicates that the signals around 13.3 ppm is adsorbed on more acidic sites than those around 14.7 ppm. The signals around 16 ppm are assigned to TMPO interacting with Na$^+$ ions and/or the framework.

The ^{13}C signals in Z5-25H (1.64 mmol/g) are located in a relatively narrow region around 18 ppm, although the ^{31}P signal spreads between 80 and 40 ppm. In general, the methyl ^{13}C chemical shift increases when the methyl group is confined in a smaller space [24–26]. In fact, crystalline TMPO has a large chemical shift because molecules are packed compactly in the crystalline state. The loading level in the above sample is high, and thus TMPO molecules are crowded in the micropores. This crowdedness confines the TMPO molecules in a small space. On the other hand, the ^{13}C chemical shift of 15–13 ppm suggests that the methyl group has a relatively large free space around it, though TMPO is adsorbed on Brønsted acid site.

4. Conclusions

Acid properties of ZSM-5 type zeolite have been studied by solid-state NMR using trimethylphosphine oxide as a probe molecule. TMPO is introduced from the gas phase at 373 K. The effect of the remaining solvent is neglected, as demonstrated by ^{1}H MAS NMR. The amounts of the loaded TMPO are quantified by the signal intensity of ^{1}H MAS NMR spectra, which are compared with the number of Brønsted acid sites estimated by ^{29}Si MAS NMR spectra through the Si/A ratio of the framework as well as by ^{27}Al MAS NMR spectra. The use of 373 K for loading the probe molecules instead of room temperature in the previous study [15,17] increases the loading level and thus almost all the acid sites are probed. The loading conditions accelerate the diffusion of the probe molecules in the micropores. ^{31}P NMR spectra of the adsorbed TMPO are traced successfully, and are interpreted by the assistance of dependences on the TMPO concentration, on the Si/Al ratio of the framework and on the cation type. The ^{31}P chemical shift in the range between 90 and 60 ppm is attributed to TMPO adsorbed on Brønsted acid sites, whereas the signal between 60 and 40 ppm is ascribed to TMPO adsorbed on other sites than Brønsted acid sites. The latter is interacting with Na$^+$ ions and/or the framework. The ^{13}C chemical shift of methyl groups in the adsorbed TMPO depends mainly on the confined space as well as on the acid strength.

Appendix A. Supplementary data

Supplementary data associated with this article can be found, in the online version, at http://dx.doi.org/10.1016/j.micromeso.2013.11.047.

References

[1] L. Baltusis, J.S. Frye, G.E. Maciel, J. Am. Chem. Soc. 108 (1986) 7119.
[2] E.F. Rakiewicz, A.W. Peters, R.F. Wormsbecher, K.J. Sutovich, K.T. Mueller, J. Phys. Chem. B 102 (1998) 2890.
[3] K.J. Sutovich, A.W. Peters, E.F. Rakiewicz, R.F. Wormsbecher, S.M. Mattingly, K.T. Mueller, J. Catalysis 183 (1999) 155.
[4] F. Haw, J. Zhang, K. Shimizu, T.N. Venkatraman, D.-P. Luigi, W. Song, D.H. Barich, J.B. Nicholas, J. Am. Chem. Soc. 122 (2000) 12561.
[5] H.-M. Kao, C.-Y. Yu, M.-C. Yeh, Microporous Mesoporous. Mater. 53 (2002) 1.
[6] Q. Zhao, W.-H. Chen, S.-J. Huang, Y.-C. Wu, H.-K. Lee, S.-B. Liu, J. Phys. Chem. B 106 (2002) 4462.
[7] A. Zheng, L. Chen, J. Yang, M. Zhang, Y. Su, Y. Yue, C. Ye, F. Deng, J. Phys. Chem. B 109 (2005) 24273.
[8] J. Wang, N. Yu, A. Zheng, J. Yang, D. Wu, Y. Sun, C. Ye, F. Deng, Microporous Mesoporous Mater. 89 (2006) 219.
[9] W. Hu, Q. Luo, Y. Su, L. Chen, Y. Yue, C. Ye, F. Deng, Microporous Mesoporous Mater. 92 (2006) 22.
[10] H.-M. Kao, P.-C. Chang, Y.-W. Liao, L.-P. Lee, C.-H. Chien, Microporous Mesoporous Mater. 114 (2008) 352.
[11] M. Okamura, A. Takagaki, M. Toda, J.N. Kondo, K. Domen, T. Tatsumi, M. Hara, S. Hayashi, Chem. Mater. 18 (2006) 3039.
[12] C. Tagusagawa, A. Takagaki, S. Hayashi, K. Domen, J. Am. Chem. Soc. 139 (2008) 7230.
[13] A. Zheng, H. Zhang, X. Lu, S.-B. Liu, F. Deng, J. Phys. Chem. B 112 (2008) 4496.
[14] A. Zheng, S.-J. Huang, W.-H. Chen, P.-H. Wu, H. Zhang, H.-K. Lee, L.-C. Ménorval, F. Deng, S.-B. Liu, J. Phys. Chem. A 112 (2008) 7349.
[15] S. Hayashi, Chem. Lett. 38 (2009) 960.
[16] N. Kojima, S. Hayashi, Bull. Chem. Soc. Jpn. 84 (2011) 1090.
[17] S. Hayashi, N. Kojima, Microporous Mesoporous Mater. 141 (2011) 49.
[18] Atlas of zeolite framework types, in: Ch. Baerlocher, W.M. Meier, D.H. Olson (Eds.), 5th ed., Elsevier, Amsterdam, 2001.
[19] S. Hayashi, Anal. Sci. 25 (2009) 133.
[20] D. Fenzke, D. Freude, T. Fröhlich, J. Haase, Chem. Phys. Lett. 111 (1984) 171.
[21] S. Hayashi, K. Hayamizu, Bull. Chem. Soc. Jpn. 64 (1991) 685.
[22] S. Hayashi, K. Hayamizu, Bull. Chem. Soc. Jpn. 62 (1989) 2429.
[23] S. Hayashi, M. Mizuno, Solid State Commun. 132 (2004) 443.
[24] S. Hayashi, K. Suzuki, K. Hayamizu, J. Chem. Soc., Faraday Trans. 1 (85) (1989) 2973.
[25] S. Hayashi, E. Akiba, Chem. Phys. Lett. 226 (1994) 495.
[26] S. Hayashi, J. Phys. Chem. 99 (1995) 7120.